ISPRS Journal of Photogrammetry and Remote Sensing 88 (2014) 91–100

Contents lists available at ScienceDirect

ISPRS Journal of Photogrammetry and Remote Sensing

journal homepage: www.elsevier.com/locate/isprsjprs

Remotely sensed biomass over steep slopes: An evaluation among successional stands of the Atlantic Forest, Brazil

Jomar Magalhães Barbosa [a,*], Ignacio Melendez-Pastor [b], Jose Navarro-Pedreño [b], Marisa Dantas Bitencourt [a]

[a] Department of Ecology, Institute of Biosciences, University of São Paulo, Brazil
[b] Department of Agrochemistry and Environment, University Miguel Hernández of Elche, Spain

ARTICLE INFO

Article history:
Received 4 October 2012
Received in revised form 9 November 2013
Accepted 19 November 2013
Available online 27 December 2013

Keywords:
Aboveground biomass
Forest succession
Tropical forest
Steep slope
Remote sensing

ABSTRACT

Remotely sensed images have been widely used to model biomass and carbon content on large spatial scales. Nevertheless, modeling biomass using remotely sensed data from steep slopes is still poorly understood. We investigated how topographical features affect biomass estimation using remotely sensed data and how such estimates can be used in the characterization of successional stands in the Atlantic Rainforest in southeastern Brazil. We estimated forest biomass using a modeling approach that included the use of both satellite data (LANDSAT) and topographic features derived from a digital elevation model (TOPODATA). Biomass estimations exhibited low error predictions (Adj. $R^2 = 0.67$ and RMSE = 35 Mg/ha) when combining satellite data with a secondary geomorphometric variable, the illumination factor, which is based on hill shading patterns. This improved biomass prediction helped us to determine carbon stock in different forest successional stands. Our results provide an important source of modeling information about large-scale biomass in remaining forests over steep slopes.

1. Introduction

Defining the spatial distribution of forest biomass enables us to evaluate how forested areas respond to human impact (Tangki and Chappell, 2008; Asner et al., 2010) and environmental conditions (Saatchi et al., 2007; Asner et al., 2009). Forest biomass is important to the carbon cycle (IPCC, 2006, 2010) because the rates of deforestation and forest regrowth determine the dynamics between carbon sources and sinks from the atmosphere (Freedman et al., 2009; Eckert et al., 2011). In this context, aboveground biomass (AGB) estimated at landscape scale presents an attractive tool for use on the evaluation of how forested regions influence the atmospheric carbon balance (Lu, 2006; Tangki and Chappell, 2008; Anaya et al., 2009; Li et al., 2010; Hall et al., 2011; Hudak et al., 2012). Regional or global AGB estimations have been largely done using a combination of field and remotely sensed data. Despite increasing interest in AGB data, some forest types, such as the Brazilian Atlantic Forest (BAF), have few studies that model their biomass using remote sensing methods (Freitas et al., 2005).

The BAF is one of the largest biodiversity centers in the world (Myers et al., 2000; Dirzo and Raven, 2003). However, 86% of its original area was deforested, which represents a reduction of approximately 129 million ha of forest area (SOS Mata Atlântica/INPE, 2012). This deforestation process occurred within multiple economic cycles (Dean, 1996). Some researchers have reported the regrowth of secondary forests in the BAF (Baptista and Rudel, 2006; Baptista, 2008; Lira et al., 2012). Although these studies are restricted both spatially and by scale, this tendency for regrowth has been explained by agricultural displacement from the BAF to the Amazon region (Pfaff and Walker, 2010; Walker, 2012).

The difficulty accessing steeply sloped areas helped maintain the remaining Atlantic forest in Brazil (Munroe et al., 2007; Teixeira et al., 2009). Similar de facto access restriction occurs in numerous other tropical mountain forests (Southworth and Tucker, 2001). Surveying the biomass in these mountainous regions is laborious, expensive and time consuming (Lu, 2006). Some success has been reported with estimating the AGB of steep-slope areas using remote sensing methods (Soenen et al., 2010; Sun et al., 2002; He et al., 2012). However, the estimation error remains high due to the difficulty of minimizing satellite data distortion in areas with heterogeneous topography (Liu et al., 2008). The combined difficulties of field surveys and satellite data processing in mountainous regions create the need for alternative field survey

* Corresponding author. Address: Rua do Matão, 101, travessa 14, 05508-900 São Paulo, SP, Brazil. Tel.: +55 1193383359; fax: +55 1130918096.
E-mail addresses: jomarmbarbosa@gmail.com (J.M. Barbosa), imelpas@gmail.com (I. Melendez-Pastor), jonavar@umh.es (J. Navarro-Pedreño), tencourt@usp.br (M.D. Bitencourt).

0924-2716/$ - see front matter © 2013 International Society for Photogrammetry and Remote Sensing, Inc. (ISPRS) Published by Elsevier B.V. All rights reserved.
http://dx.doi.org/10.1016/j.isprsjprs.2013.11.019

strategies and new statistical approaches to modeling biomass (Soenen et al., 2010).

In this study, we investigated how topographical features affect biomass estimations from remotely sensed data using different modeling steps. We also evaluated the accuracy of the biomass estimations through forest successional stands. The topographic information was included on the modeling steps to analyze its influence on the biomass estimation. In addition, we compared the spatial pattern of the modeled biomass among the successional forest stands. The results provided both a straightforward framework and a novel method for determining forest biomass in steep slope regions.

2. Materials and methods

2.1. Study area

The study area is located in Vale do Ribeira at São Paulo State, southern Brazil (24°33′S and 48°39′W; Fig. 1). It covers approximately 15,000 ha and encompasses elevations from 100 m to 900 m, slopes ranging from 0° to 40°, and a full variety of terrain aspects. This area is a representative portion of the topographic characteristics of the largest remaining Brazilian Atlantic Forest. The climate is characterized by consistent rainfall throughout the year, with an average annual rainfall about 2000 mm and a mean annual temperature of over 21 °C. The vegetation consists of ombrophilous tropical forests, which have approximately 100–160 species per hectare (Tabarelli and Mantovani, 1999) and a complex biophysical structure (Guilherme et al., 2004; Marques et al., 2009). Steep slopes within the study area have reduced deforestation required for intensive land use practices (Teixeira et al., 2009). Historically, major forest disturbances occurred through the slash and burn agriculture system, which was practiced by small farmers (Adams, 2000; Peroni and Hanazaki, 2002). This historical land management formed forest mosaics that include primary and secondary forests in different stages of regrowth.

2.2. Vegetation field data

Vegetation field data were collected in November 2010. A first survey (S1) of 170 points was distributed inside 17 plots of 0.36 ha. This number and area of calibration plots (totaling 6.12 ha) is similar to previous biomass mapping of tropical forests (Cutler et al., 2012). For each plot, 10 non-overlapping sample points were randomly selected and surveyed via the point-centered quarter method (PCQ) (Cottam and Curtis, 1956). The center of each sample point was divided into four quadrants. Subsequently, the nearest tree with a diameter at breast height (DBH) of over 4.9 cm in each quadrant was selected, and its total height, DBH and distance to the sample point were measured, totaling 40 trees for each plot (Fig. 2). Distance and tree height measurements were taken with a laser distance meter (Leica DISTRO A5). The stand density at each plot (S) was calculated as follows:

$$S_i = 4/(d_1^2 + d_2^2 + d_3^2 + d_4^2) \quad (1)$$

$$S = \Sigma S_i/n \quad (2)$$

where S_i is a tree density estimate for the ith sampled point; d_1, d_2, d_3 and d_4 are the distances (m) from the central point to the nearest tree in each quadrant; n is the number of points. S is the mean tree

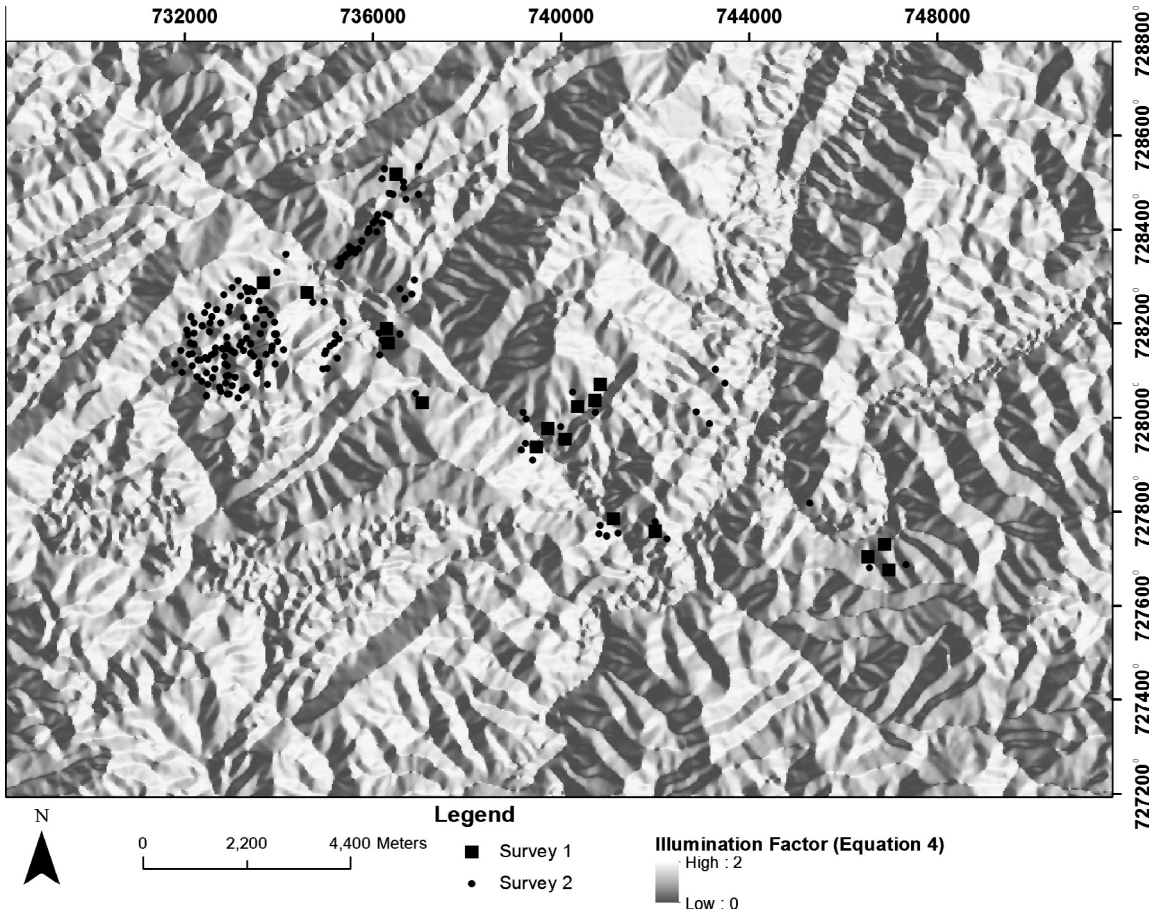

Fig. 1. Study area and surveyed points. The Illumination Factor represents a relief enhancement of solar illumination differences between mountainsides.

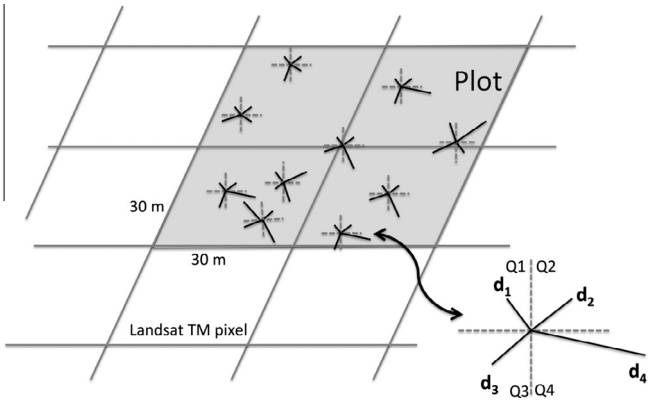

Fig. 2. Sample design of the point quadrant method. Ten sampled points were scattered within the plot (Adapted from Main-Knorn et al., 2011). Q_1, Q_2, Q_3, Q_4 are quadrants and d_1, d_2, d_3 and d_4 are the distances (m) of the central point to the nearest tree (DBH over 10 cm) in each quadrant.

density considering n surveyed points, which is subsequently extrapolated to the plot area (0.36 ha) and then to one hectare.

The stand tree density was multiplied by the mean AGB of each sampled plot. The AGB of the sampled trees was estimated using an allometric equation (Eq. (3)) calibrated with dry biomass from tree leaves, branches and trunks (Burger and Deletti, 2008). This equation was used due to the structural similarity between our study area and that used by the authors:

$$\mathrm{Ln}(\mathrm{AGB}_i) = -3.676 + 0.951\mathrm{Ln}(\mathrm{DBH}^2 h) \quad (3)$$

where AGB_i is the dry aboveground biomass (kg) of the tree, DBH is the diameter at breast height (cm), and h is the total tree height (m). A general biomass-carbon conversion factor of 47.4% (±2.51% SD) was used despite the fact that generic conversion factors lead to overestimates of biomass resulting from high interspecific variation in wood C content (Martin and Thomas, 2011).

A second sample was taken for use in the validation procedure. For this second survey (S2), another 174 points were scattered over the study area (Fig. 1) and biomass was estimated for each forest succession class using the same PCQ protocol. Subsequently, the biomass data from the plots (S1) and the scattered points (S2) were statistically compared. Both surveys, S1 and S2 (totaling 344 sampled points) were scattered over the study area using a stratified protocol that included three illumination factor ($\mathrm{IF}_{\mathrm{hillshading}}$) and two forest succession classes (see classifications in Section 2.3). This sampling protocol allowed different combination of forest types, aspects and slope to be surveyed. Specifically, 34% of the total sampled points were located on the initial secondary forest and 66% on advanced secondary forest. In addition, all aspects were proportionally surveyed (24% on the north, 22% south, 26% east and 28% west). Thirty-seven percent of the sampled points were located on slopes below 20° and 63% on slopes steeper than 20°.

2.3. Topographic and image data processing

Topographic data was employed for satellite imagery preprocessing and also for biomass prediction. The terrain data were acquired using a digital elevation model (DEM). The DEM was obtained from TOPODATA (http://www.dsr.inpe.br/topodata), a Brazilian geomorphometric database (Valeriano et al., 2006; Valeriano, 2008). TOPODATA is available for the entirety of Brazil and has been refined to 1 arcsec (~30 m) resolution through a geostatistical approach using the Shuttle Radar Topography Mission dataset (Valeriano and Albuquerque, 2010; Valeriano and Rossetti, 2012). Resampling the DEMs with geostatistical approaches, such as on the TOPODATA, produces satisfactory estimates of geomorphometric data even though it does not increase the level of detail (Grohmann and Steiner, 2008; Mantelli et al., 2011). Instead, this technique preserves the coherence of the angular properties (i.e., slope and aspect) of neighboring pixels (Valeriano et al., 2006) and can be an important source of data in regions where original 1 arcsec DEM is unavailable.

The DEM and solar angles from the same time as the Landsat data, solar azimuth (84.89°) and zenith (27.37°), were used to obtain an illumination factor (IF) image (Fig. 1). The IF is the angle between the normal of the pixel surface and the solar zenith direction, which represents a relief enhancement used to identify hill sides shadowed in a certain sun elevation and azimuth (Canavesi, 2008; Valeriano and Albuquerque, 2010; Valeriano, 2011). The IF was used in the present study as an explanatory variable of the modeling biomass.

Using spherical trigonometry, the IF was calculated in three separate ways: {1} using a hillshade variable (considering the direction of the ground, slope, solar azimuth, and solar zenith (Eq. (4)) (Canavesi, 2008); {2} using a sum of orthogonal vectors (Eq. (5)) (Canavesi and Ponzoni, 2007; Valeriano and Albuquerque, 2010); and {3} using the law of cosines (Eq. (6)) (Slater, 1980; Valeriano, 2011):

$$\mathrm{IF}_{\mathrm{hillshading}} = \sqrt{(\cos(\varphi_{x,y} - \varphi_s) + \cos(\theta_{x,y} - \theta_s))^2} \quad (4)$$

$$\mathrm{IF}_{\mathrm{vector\ sum}} = (\cos(\varphi_{x,y} - \varphi_s))^2 + (\cos(\theta_{x,y} - \theta_s))^2 \quad (5)$$

$$\mathrm{IF}_{\cos} = \cos\theta_{x,y}\cos\theta_s + \sin\theta_{x,y}\sin\theta_s\cos(\varphi_{x,y} - \varphi_s) \quad (6)$$

where IF is the illumination factor image (scaled from 0 to 2), $\varphi_{x,y}$ the aspect, φ_s the solar azimuth, $\theta_{x,y}$ the slope, and θ_s is the solar zenith. The last four variables are expressed in degrees. Aspect and slope variables were obtained from the DEM.

In addition to the topographical data (IF, slope, aspect), Landsat Thematic Mapper (TM) satellite imagery (path 220 and row 77) was also used as an explanatory variable in the biomass estimation. The acquisition date of the TM data was November 19, 2010, which is the same period of the field survey. First, the level-1 TM data were converted from digital numbers to a spectral radiance using published calibration gain and offset values (Chander et al., 2010). The image bands were then converted to top of atmosphere reflectance and atmospherically corrected based on the COS-T1 model, which considers the earth-sun distance, mean exoatmospheric solar irradiance, solar zenith angle and dark object subtraction (Chavez, 1996; Lu et al., 2002). Then, two different topographic correction methods were applied to the TM images in order to evaluate their suitability for the biomass estimates, namely the C-correction (Teillet et al., 1982) and the SCS + C correction (Soenen et al., 2005). The SCS + C correction is based on the photometric Sun-Canopy-Sensor (SCS) method and theoretically preserves geotropic nature of the vertical tree growth and performs better than the C-correction (Soenen et al., 2005, 2010).

Biomass modeling with satellite imagery was done using separate TM bands and with vegetation indices, such as the normalized difference vegetation index (NDVI) and enhanced vegetation index (EVI). The NDVI was calculated as (near infrared − red)/(near infrared + red) and the EVI was calculated as (near infrared − red)/(near infrared + 6 × red−7.5 × blue + 1) (Huete et al., 1997).

The TM data were also used to elaborate a land cover classification map focusing on successional forest stands. An unsupervised classification with the k-means clustering algorithm using all of TM bands was applied. Six land cover classes were identified: the initial secondary forest (highest trees less than 10 m height), the advanced secondary forest (highest trees over 10 m height), urban sites, anthropic settlements (productive fields, pasture), abandoned

anthropic settlements and water. Advanced secondary forest and primary forest stands were grouped into the same class due their great spectral similarity as observed in the image-based spectral signatures. The map accuracy was assessed using a 200 points validation dataset by computing the Kappa coefficient (Pontius, 2000). This land cover validation dataset encompassed 100 field-georeferenced ground truth points and another 100 points obtained from ALOS imaging (date 2010 and 10 m spatial resolution) and SPOT images from Google Earth® (date 2010).

2.4. Predictive biomass modeling

The biomass was estimated using a set of input data, such as the Landsat reflectance (TM1, TM2, TM3, TM4, TM7 bands), NDVI, EVI, and topographic variables, such as IF, slope, and aspect (Fig. 3). Landsat data was analyzed considering both the topographically corrected and uncorrected images. The modeling was processed using generalized linear models (GLM) by linking the averages of the spatially coinciding satellite data to each plot sampled in the biomass field survey (S1). The GLM is commonly used in environmental research (Guisan and Zimmermann, 2000) and has been increasingly popular in remote sensing (Schwarz and Zimmermann, 2005; Mathys et al., 2009; Kajisa et al., 2009) because it allows for non-linear and non-constant variance structures in the data (Bolker, 2008). To avoid multicollinearity amongst the explanatory variables, the variation inflation factor (VIF) and tolerance (O'Brien, 2007) were used to define any correlations. The VIF and tolerance were calculated from Eqs. (7) and (8), respectively:

$$\mathrm{VIF} = 1/1 - R^2 \tag{7}$$

$$\mathrm{Tolerance} = 1/\mathrm{VIF} \tag{8}$$

The biomass model plausibility was evaluated using the Akaike's Information Criterion (AIC) (Akaike, 1974) and *R*-squared. Models with ΔAIC values less than or equal to 2 were considered equally plausible. We also used the Akaike weights to indicate the probability that the model was the best of the candidate models (McCullagh and Nelder, 1989). All of the modeling steps were implemented using the statistical programming language R version 2.0.0 (Development Core Team, 2011).

2.5. Estimated AGB versus field data

The error estimation of the predicted biomass was calculated using the root mean square error (RMSE) between the observed (field) and modeled data. In this validation procedure, we randomly selected 70% of the total data sets from 17 plots one hundred times. For each selection, the RMSE between the remaining 30% field biomass values and the model estimates was obtained. Next, the reliability of each model using the mean of the 100 RMSE values was evaluated. Finally, the bias trends of the models from the percent error for 1000 comparisons between the observed and predicted data were analyzed. These comparisons allowed any positive or negative trends in the errors to be detected.

To ensure that the biomass estimated using the plot data was representative of the entire study area, the modeled data was compared with the S2 validation sample. First, the average modeled AGB for 20 polygons (0.81 ha each) randomly distributed over each forest succession class was obtained and then compared to the field biomass from S2. Both the field and modeled biomass were statistically compared for each forest class using their means and standard deviations. The highest similarity between the field and modeled data represents the highest feasibility of the modeled biomass.

3. Results

3.1. Field forest structure

The forest stand parameters corresponding to the 344 surveyed points (S1 and S2) are shown in Table 1. The average AGB in the studied area was 107 Mg/ha. There were 227 (66%) sampled points in the advanced secondary forest stand, with mean biomass of

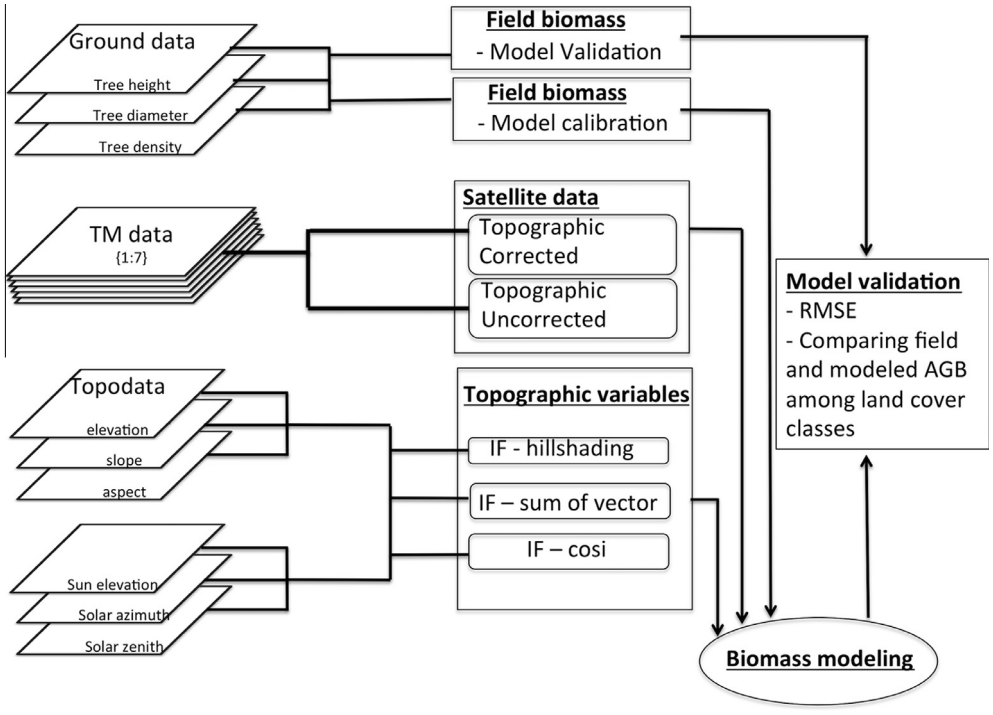

Fig. 3. Procedure for predicting the biomass from the TM, inventory plot and topographic data.

Table 1
Summary of the mean (± standard deviation) forest stand parameters for each forest successional class.

Successional stage	Tree diameter (cm)	Tree height (m)	Tree density (ind./ha)	Biomass (Mg/ha)
Initial	10 (±4)	7 (±2)	2084 (±1927)	54 (±68)
Advanced	14 (±5)	9 (±2)	2185 (±1306)	128 (±190)
Total	13 (±5)	8 (±2)	2144 (±1491)	107 (±170)

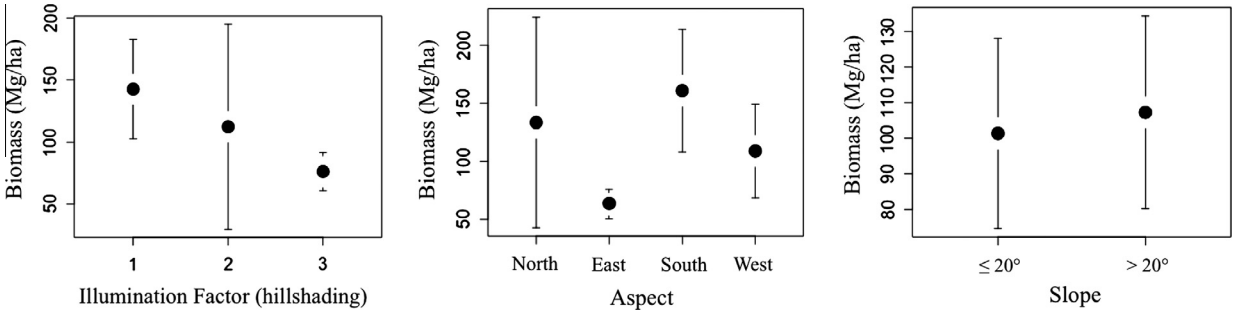

Fig. 4. Mean modeled biomass and confidence intervals (95%) related to Illumination Factor (IF), aspect and slope. The IF was classified as 1 = IF from 0 to 0.66; 2 = IF from 0.66 to 1.33; and 3 = IF from 1.33 to 2. The aspect was classified as North = ground directions from 0° to 45° and 316° to 360°; East = 46° to 135°; South = 136° to 225°; and West = 226° to 315°.

Table 2
Summary of the suitability of the models. ΔAIC_c = Akaike Information Criterion, Adj. R^2 = Adjusted coefficient of determination, RMSE = root mean square error, AGB = aboveground biomass, TM5 = mid-infrared Landsat TM, IF = Illumination Factor. The models used the identity link-function.

Model	Fitting parameters				Values			
	ΔAIC_c	Weight	Adj. R^2	RMSE (Mg/ha)	Variable name	Estimate (β)	Std. Err. (β)	ρ-Level
Model 1	0.0	0.95	0.67	35	Intercept	−6.04644	1.83352	0.0050
					Ln(TM5)	−5.44825	0.95790	0.0001
					Ln(TM5) × Ln($IF_{hillshading}$)	−0.22188	0.05939	0.0022
Model 2	6.5	0.036	0.52	52	Intercept	−1.1382	1.3758	0.4219
					Ln(TM5)	−3.0333	0.7122	0.0007
					Ln(TM5) × Ln($IF_{vectorsum}$)	1.2074	0.5378	0.0414
Model 3	7.9	0.017	0.40	60	Intercept	−7.736	3.575	0.0470
					Ln(TM5 SCS-C correction)	−6.143	1.801	0.0038
Model 4	9.0	0.010	0.44	63	Intercept	−0.464	1.45999	0.7553
					Ln(TM5)	−1.684	0.90784	0.0848
					Ln(slope) × Ln(aspect)	0.096	0.06098	0.1353
Model 5	10.2	0.005	0.39	62	Intercept	−4.5288	3.7172	0.2432
					Ln(TM5)	−4.7679	2.0757	0.0376
					Ln(TM5) × Ln(IF_{cos})	−0.9651	0.8388	0.2692
Model 6	11.8	0.002	0.24	59	Intercept	−6.116	4.227	0.1685
					Ln(TM5 C correction)	−5.579	2.231	0.0245
Null model	14.7	<0.001						

128 Mg/ha, and 117 points (34%) in the initial secondary forest stand, with mean biomass of 54 Mg/ha. The low global mean AGB is due the inclusion in the sample of secondary forest in different successional stands. The high standard deviation of the mean biomass (Table 1) indicates the large range of biomass values surveyed for each class. This large forest structure variation within the sampled data ensures that different forest succession stages were included in the modeling procedure.

3.2. Topographic patterns

The relief pattern of the studied area forms a complex mosaic of slopes and aspects. Different combinations of slopes and aspects were synthetized into three illumination factors (IF_{cos}, $IF_{hillshading}$ and $IF_{vector\ sum}$). The IF_{cos} and $IF_{hillshading}$ showed higher values when the related slope aspect was similar to the sun azimuth of 84° (sun angle at the acquisition time of the Landsat TM data used in present study). Contrarily, the IF_{vector} sum exhibited two peaks of maximum IF relating to the aspect. The upper and lower limits of $IF_{hillshading}$ values were found in many slope degrees as well as $IF_{vector\ sum}$, while IF_{cos} values showed higher heterogeneity in sloped areas then flat areas.

A negative, though weak, relation between the biomass and the $IF_{hillshading}$ ($r = -0.32$; $\rho = 0.004$) indicated a tendency for elevated biomass values in areas with low illumination factor (Fig. 4). Intermediary IF values showed a large range of biomass resulting in the weak relationship between both variables. In addition, the forest biomass showed a weak positive correlation with the aspect ($r = 0.30$; $\rho = 0.006$) and no correlation with the slope (Fig. 4).

3.3. Modeling biomass using both field and remotely sensed data

One model was a plausible predictor of forest AGB ($\Delta AIC_c < 2$). - Table 2 summarizes the six best models in relation to the null model. Some explanatory variables, such as the NDVI and EVI, were

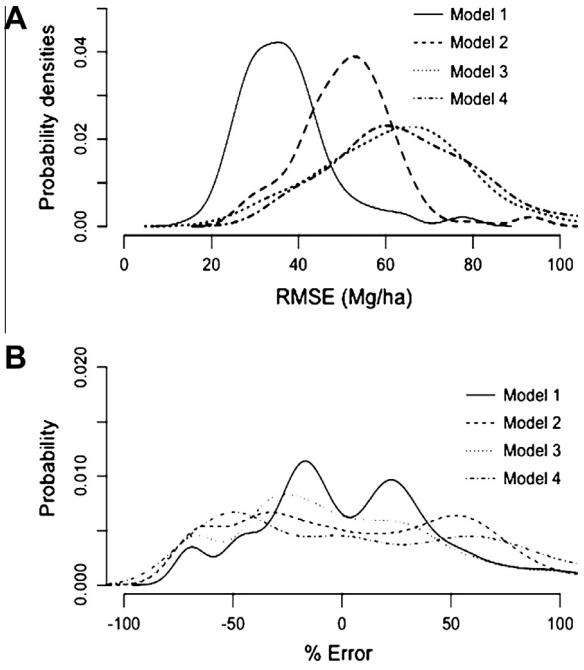

Fig. 5. Histogram of the probability densities of the best four models for (a) the randomized RMSE and (b) for bias tendencies using the error percentage. The model numbers are the same for both figures as in Table 2. The histograms were normalized.

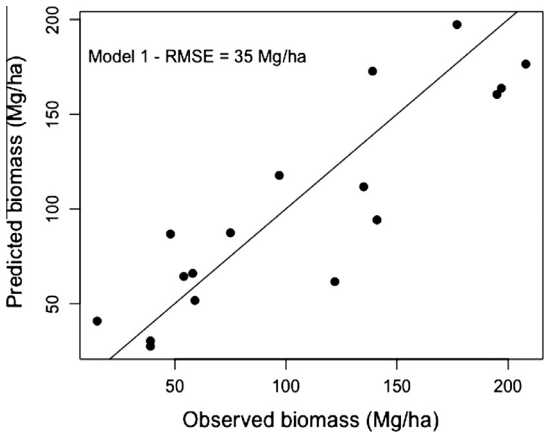

Fig. 6. The relationship between the observed biomass and that predicted by the GLM defined in model 1 [$Ln(AGB) = -6 - 5.4(Ln(TM5)) - 0.2(Ln(TM5) \times Ln(IF_{hillshading}))$].

not shown due to their poor predictions. The model that combined the topographically uncorrected Landsat TM5 (1.55–1.75 μm) and IFhillshading was the most predictive for AGB ($R^2 = 0.67$; RMSE = 35 Mg/ha). This model had a reduced probability of finding large errors (Fig. 5a) and showed two error peaks of approximately 25% for both the negative and positive tendencies (Fig. 5b). The relationship between the predicted and observed AGB for this model is shown in Fig. 6. The multicollinearity test for model 1 indicates a VIF of 2.9 and a tolerance of 0.34.

The estimated biomass within 20 polygons (0.81 ha each) randomly scattered in each of the forest succession class were 50.3 Mg/ha (SD = 17 Mg/ha) for the initial secondary forest and 172.7 Mg/ha (SD = 66 Mg/ha) for the advanced secondary forest. These modeled data were closely related to the scattered field survey points (S2), which showed a mean field biomass of 54 Mg/ha

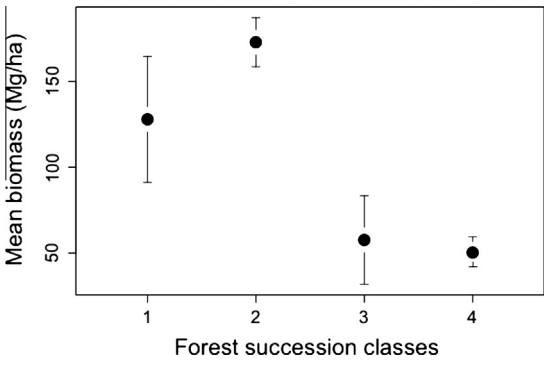

Fig. 7. Mean biomass and confidence intervals (95%). 1: Field biomass in the advanced forest class. 2: Modeled biomass in the advanced forest class. 3: Field biomass in the initial forest class. 4: Modeled biomass in the initial forest class.

(SD = 68 Mg/ha) for the initial secondary forest and 128 Mg/ha (SD = 190 Mg/ha) for the advanced secondary forest class (Fig. 7). There were no statistically significant differences between these field-based data and the modeled data ($\rho < 0.05$). While the estimated biomass of the initial forest succession class possessed low heterogeneity, the advanced forest class showed high variance in the modeled biomass of randomly selected plots (Fig. 8). The advanced forest succession class showed higher differences for the modeled biomass both between the plots and within each plot.

The land-cover map (Fig. 9) resulted in an overall kappa of 0.80 (Congalton, 1991). Although this accuracy was acceptable, the error matrix merges the initial secondary forests with abandoned settlements. As illustrated in Table 3, the studied region had a large forested area (76.4% of the total area). The sum of all human settlements represented a 22.75% of the studied area (pasture, subsistence agriculture, urban, and abandoned settlements). The best biomass model indicated approximately 23.8 (±1.25) TC/ha and 81.8 (±4.33) TC/ha for the initial secondary forest and advanced secondary classes, respectively. The biomass maps for the initial and advanced forest classes developed using model 1 demonstrated different visual patterns (Fig. 9). Considering the forested area of each land cover class, the studied landscape stored more than 5 million T of aboveground forest carbon.

4. Discussion

The results indicate a high importance of the topographic pattern on the aboveground biomass modeling. For the studied Brazilian Atlantic Forest area, the best biomass prediction occurred when we combined a satellite image of the Landsat TM5 (1.55–1.75 μm) band with a secondary geomorphometric variable, the illumination factor (IF). Among three IF indices tested, models that integrated $IF_{hillshading}$ and TM5 band resulted in best biomass predictions. $IF_{hillshading}$ provides a snapshot of the solar illumination at the moment of the TM data acquisition, enhancing illumination differences between mountainsides (Canavesi, 2008; Valeriano and Albuquerque, 2010; Valeriano, 2011). In addition, different $IF_{hillshading}$ values, with specific aspects and slopes, showed characteristic vegetation covers. For example, low $IF_{hillshading}$ coincided with high values of forest biomass and it mainly occurred in sloping hills facing to the west and south, which are areas with low illumination in the southern hemisphere. This tendency is probably related to the maintenance of an elevated biomass in shaded and inaccessible areas that experienced less historical agriculture usage (Munroe et al., 2007; Silva et al., 2008; Teixeira et al., 2009).

$IF_{hillshading}$ enhances differences of solar reflectance due steep slope patterns and correlates with the vegetation cover, thereby

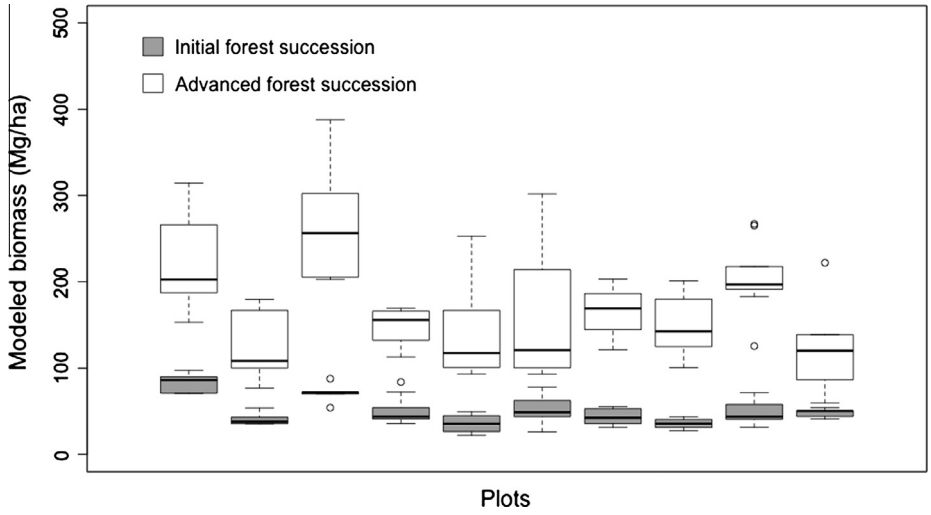

Fig. 8. Boxplot of the mean modeled biomass over 20 plots (0.81 ha each) randomly scattered throughout the landscape and comprising both the initial and advanced forest succession classes.

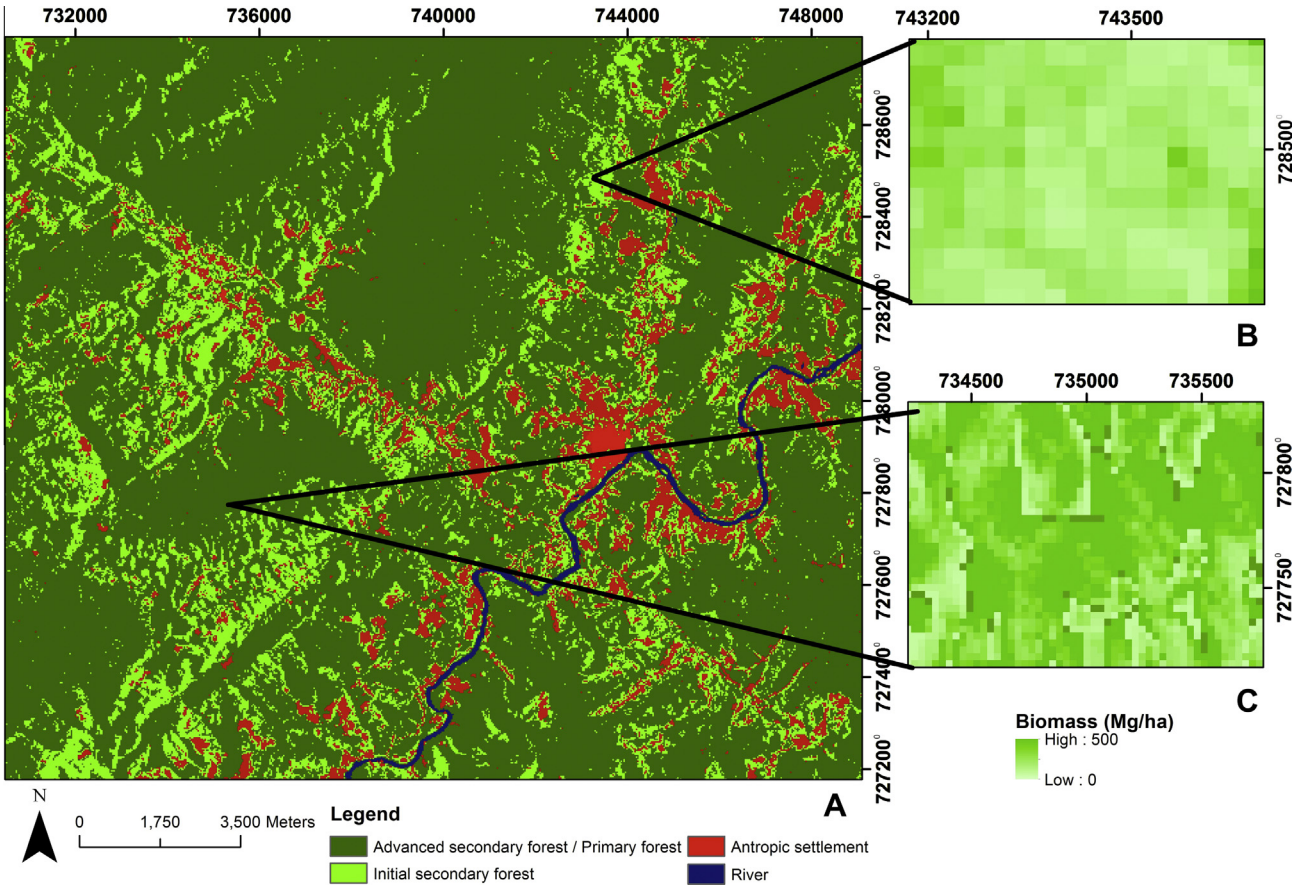

Fig. 9. Land-cover and biomass maps of the studied area. (A) Land-cover, (B) initial secondary forest and (C) advanced secondary forest. Biomass predictions elaborated using the model (model 1).

improving the accuracy of AGB predictions. Biomass and terrain variables are usually correlated, as shown by previous studies (Sun et al., 2002; He et al., 2012; Dahlin et al., 2012). Therefore, both the explicit parameterization of the sun reflection geometry and the inclusion of topographic data in the model are alternatives to refine biomass predictions (Soenen et al., 2010; Main-Knorn et al., 2011). However, our predictions were weak when we used slope and aspect independently or when we used topographically corrected images.

Early topographic correction, such as the C-correction (Teillet et al., 1982), has been reported to be capable of reducing the topographic effects to a certain degree, but only for highly non-Lambertian surfaces (Wu et al., 2008). A more recent topographic correction approach, the SCS + C (Soenen et al., 2005), is more concise and compensates for changes in the self-shadowed area across

Table 3
Area for each land-cover class.

Land cover	ha	%
Water	746.4	0.83
Anthropic settlement	12958.4	14.53
Urban	104.3	0.11
Abandoned anthropic settlement	7238.7	8.11
Initial secondary forest	8216.4	9.21
Advanced secondary forest/primary forest	59934.1	67.19

Overall Kappa = 0.8.

the range of canopy complexities (Kane et al., 2008). However, our results suggest that both topographic corrections do not perform well with our datasets, which is possibly because of the intricate orography and complexity of the forest stands. The topographic correction of the satellite images was based on the assumption that there was a linear relationship between the sun reflectance and the cosine of the angle between the normal of the ground and the solar beam (Ekstrand, 1996). Nevertheless, the scatterplot of both variables failed to generate a suitable linear regression, resulting in the low performance of the corrected images in predicting biomass.

Recent remote sensing biomass estimates of tropical forests employ images from active sensors such as RADAR or LIDAR (Englhart et al., 2011; Saatchi et al., 2011), while others employ passive optical systems (Tangki and Chappell, 2008; Kajisa et al., 2009; Li et al., 2010; Wijaya et al., 2010; Sarker and Nichol, 2011) or a combination of both (Bitencourt et al., 2007; Wang and Qi, 2008; Cutler et al., 2012). In the present study, we used passive optical systems, which provide a large pool of data suitable for biomass mapping because they are widely available for many regions and time sets (i.e. historical images from Landsat program). However, cloud coverage in tropical regions and satellite data saturation are major constraints for passive optical systems when modeling tropical forest biomass (Lu, 2006). In our case, we used cloud free images. In addition, the saturation effect on our modeling procedure may be reduced because there is a lower biomass amount in the secondary BAF than in Amazon (Vieira et al., 2008; Anderson, 2012). Previous studies in tropical forests found that using mid-infrared spectral bands for biomass estimates minimized the pixel saturation (Steininger, 2000; Freitas et al., 2005). Our results agree with this statement, as demonstrated by the inclusion of the mid-infrared Landsat band (TM5) in better performing models. Nevertheless, our best-performing model still showed an important error (35 Mg/ha) that might be minimized using multisensory data or processing approaches such as multi-date and texture analyzes.

Beyond satellite image processing, field data is a determinant of the accuracy of estimates. The integration between both the point-centered quarter method and the plot-based approach for surveying forest structure shows similar results for studies limited to plot-based survey of the BAF (Alves et al., 2010; Borgo, 2010). This sample protocol allowed surveys of several locations throughout the landscape with large plots (i.e. 0.36 ha) and reduced field-work. The use of large plots permits a more representative biophysical variation of the vegetation in the sample and results in minor model inaccuracies due to GPS positional errors (Frazer et al., 2011; Zolkos et al., 2013). As demonstrated in the methods, the PCQ is an estimative method for tree density and demands an elevated number of points by forest stand (Bryant et al., 2004). In the present study, ten PCQ points within only 0.36 ha showed reliable forest structure estimates.

Differences between initial and advanced biomass occurred for both the field and modeled data (Fig. 7). These results indicate the feasibility of predicting the AGB for different forest succession stages. The modeled biomass allowed identification of structural heterogeneity inside the forest classes (Fig. 8). This finding indicates that spatially explicit AGB estimates can provide qualitative information about the forest successional stage and may be used to investigate forest regrowth when an increase in the forest area does not exist. Different authors have studied forest succession using historical analysis or stand classes (Neeff et al., 2006; Liu et al., 2008; Helmer et al., 2009; Sirén and Brondizio, 2009). However, forest age classes and stages (i.e., initial, intermediate and advanced) were not equally defined by these authors. The lack of standardization in successional stands may be a problem when comparing different studies. The species composition and forest structure such as biomass, diameter and height can be better suited to defining the successional stage (Vieira et al., 2003).

In Brazil, many remote sensing studies have been conducted in the Amazon (Foody et al., 2003; Lu et al., 2004; Li et al., 2010; d'Oliveira et al., 2012), which has resulted in the use of Amazon-based biomass estimates at the national level due to the minimal effort to measure the AGB of other biomes such as the BAF. Biomass estimates in the BAF have been previously studied with field-based methods (Vieira et al., 2008). However, few studies have measured the large-scale biomass in the BAF using remote sensing data. In this context, the present study provides important tools for inferring the biomass on steep slopes in the Atlantic forest.

5. Conclusions

This study provides a feasible framework for estimating the aboveground forest biomass in the Brazilian Atlantic Forest with reduced field requirements. In addition, the results indicate that the combination of mid-infrared spectral bands with a secondary geomorphometric variable significantly improved biomass estimates in a mountainous area. The reduced time required to calibrate the model when using the point-centered quarter method can provide an alternative survey strategy to estimate the field biomass and promote the validation of biomass maps. However, this methodology can be better evaluated using other forest types and different satellite data. Considering the scarcity of remotely sensed biomass data from the Atlantic Rainforest, our results present an important source of information about large-scale biomass estimation in this biome and demonstrate that the forests remaining on the steep slopes in the Brazilian Atlantic Forest form important carbon pools.

Acknowledgments

Coordenação de Aperfeiçoamento de Pessoal de Nível Superior (CAPES) for the scholarship. We thank Esther Sebastián González and anonymous referees for commenting on the manuscript.

Appendix A. Supplementary material

Supplementary data associated with this article can be found, in the online version, at http://dx.doi.org/10.1016/j.isprsjprs.2013.11.019. These data include Google maps of the most important areas described in this article.

References

Adams, C., 2000. As roças e o manejo da Mata Atlântica pelos caiçaras: uma revisão. Interciência 25 (3), 143–150.
Akaike, H., 1974. A new look at the statistical model identification. IEEE Trans. Autom. Control 19 (6), 716–723.
Alves, L.F., Vieira, S.A., Scaranello, M.A., Camargo, P.B., Santos, F.A.M., Joly, C.A., Martinelli, L.A., 2010. Forest structure and live aboveground biomass variation along an elevational gradient of tropical Atlantic moist forest (Brazil). For. Ecol. Manage. 260 (5), 679–691.
Anaya, J.A., Chuvieco, E., Palacios-Orueta, A., 2009. Aboveground biomass assessment in Colombia: a remote sensing approach. For. Ecol. Manage. 257 (4), 1237–1246.

Anderson, L.O., 2012. Biome-scale forest properties in Amazonia based on field and satellite observations. Remote Sens. 4 (5), 1245–1271.
Asner, G.P., Hughes, R.F., Varga, T.A., Knapp, D.E., Kennedy-Bowdoin, T., 2009. Environmental and biotic controls over aboveground biomass throughout a tropical rain forest. Ecosystems 12 (2), 261–278.
Asner, G.P., Martin, R.E., Knapp, D.E., Kennedy-Bowdoin, T., 2010. Effects of Morella faya tree invasion on aboveground carbon storage in Hawaii. Biol. Invasions 12 (3), 477–494.
Baptista, S.R., 2008. Metropolitanization and forest recovery in southern Brazil: a multiscale analysis of the Florianópolis city-region, Santa Catarina State, 1970 to 2005. Ecol. Soc. 13 (2), 5.
Baptista, S.R., Rudel, T.K., 2006. A re-emerging Atlantic forest? Urbanization, industrialization and the forest transition in Santa Catarina, southern Brazil. Environ. Conserv. 33 (3), 195–202.
Bitencourt, M.D., de Mesquita Jr., H.N., Kuntschik, G., 2007. Cerrado vegetation study using optical and radar remote sensing: two Brazilian case studies. Can. J. Remote Sens. 33 (6), 468–480.
Bolker, B.M., 2008. Ecological models and data in R. Princeton University Press, New Jersey (USA).
Borgo, M., 2010. A Floresta Atlântica do litoral norte do Paraná, Brasil: aspectos florísticos, estruturais e estoque de biomassa ao longo do processo sucessional. PhD in Forestry, Paraná Federal University, Curitiba, Brazil.
Bryant, D.M., Ducey, M.J., Innes, J.C., Lee, T.D., Eckert, R.T., Zarin, D.J., 2004. Forest community analysis and the point-centered quarter method. Plant Ecol. 175 (2), 193–203.
Burger, D.M.D., Deletti, W.B.C., 2008. Allometric models for estimating the phytomass of a secondary Atlantic Forest area of southeastern Brazil. Biota Neotropica 8 (4), 131–136.
Canavesi, V., 2008. Aplicação de dados Hyperion EO-1 no estudo de plantações de Eucalyptus spp. PhD in the Remote Sensing Department, Instituto Nacional de Pesquisas Espaciais (INPE), São José dos Campos SP, Brazil.
Canavesi, V., Ponzoni, F.J., 2007. Relações entre variáveis dendrométricas de plantios de Eucalyptus sp. e valores de FRB de superfície de imagens do sensor TM/Landsat 5. In: INPE (Ed.), XIII Simpósio Brasileiro de Sensoriamento Remoto, Instituto de Pesquisas Espaciais (INPE), Florianópolis, Brazil, pp. 1619–1625.
Chander, G., Haque, M.O., Micijevic, E., Barsi, J.A., 2010. A procedure for radiometric recalibration of Landsat 5 TM reflective-band data. IEEE Trans. Geosci. Remote Sens. 48 (1), 556–574.
Chavez, P.S., 1996. Image-based atmospheric corrections revisited and improved. Photogramm. Eng. Remote Sens. 62 (9), 1025–1036.
Congalton, R.G., 1991. A review of assessing the accuracy of classifications of remotely sensed data. Remote Sens. Environ. 37 (1), 35–46.
Cottam, G., Curtis, J.T., 1956. The use of distance measures in phytosociological sampling. Ecology 37 (3), 451–460.
Cutler, M.E.J., Boyd, D.S., Foody, G.M., Vetrivel, A., 2012. Estimating tropical forest biomass with a combination of SAR image texture and Landsat TM data: an assessment of predictions between regions. ISPRS J. Photogramm. Remote Sens. 70 (1), 66–77.
Dahlin, K.M., Asner, G.P., Field, C.B., 2012. Environmental filtering and land-use history drive patterns in biomass accumulation in a mediterranean-type landscape. Ecol. Applic. 22 (1), 104–118.
Dean, W., 1996. A Ferro e Fogo: a História da Devastação da Mata Atlântica. Companhia das Letras, São Paulo, Brazil.
Dirzo, R., Raven, P.H., 2003. Global state of biodiversity and loss. Ann. Rev. Environ. Resour. 28 (1), 137–167.
d'Oliveira, M.V.N., Reutebuch, S.E., McGaughey, R.J., Andersen, H.-E., 2012. Estimating forest biomass and identifying low-intensity logging areas using airborne scanning lidar in Antimary State Forest, Acre State, Western Brazilian Amazon. Remote Sens. Environ. 124 (1), 479–491.
Eckert, S., Ratsimba, H.R., Rakotondrasoa, L.O., Rajoelison, L.G., Ehrensperger, A., 2011. Deforestation and forest degradation monitoring and assessment of biomass and carbon stock of lowland rainforest in the Analanjirofo region, Madagascar. Forest Ecol. Manage. 262 (11), 1996–2007.
Ekstrand, S., 1996. Landsat TM-based forest damage assessment: correction for topographic effects. Photogramm. Eng. Remote Sens. 62 (2), 151–161.
Englhart, S., Keuck, V., Siegert, F., 2011. Aboveground biomass retrieval in tropical forests—the potential of combined X- and L-band SAR data use. Remote Sens. Environ. 115 (5), 1260–1271.
Foody, G.M., Boyd, D.S., Cutler, M.E.J., 2003. Predictive relations of tropical forest biomass from Landsat TM data and their transferability between regions. Remote Sens. Environ. 85 (4), 463–474.
Frazer, G.W., Magnussen, S., Wulder, M.A., Niemann, K.O., 2011. Simulated impact of sample plot size and co-registration error on the accuracy and uncertainty of LiDAR-derived estimates of forest stand biomass. Remote Sens. Environ. 115 (2), 636–649.
Freedman, B., Stinson, G., Lacoul, P., 2009. Carbon credits and the conservation of natural areas. Environ. Rev. 17 (1), 1–19.
Freitas, S.R., Mello, M.C.S., Cruz, C.B.M., 2005. Relationships between forest structure and vegetation indices in Atlantic Rainforest. For. Ecol. Manage. 218 (1–3), 353–362.
Grohmann, C.H., Steiner, S.S., 2008. SRTM resample with short distance-low nugget kriging. Int. J. Geographical Inform. Sci. 22 (8), 895–906.
Guilherme, F.A.G., Morellato, L.P.C., Assis, M.A., 2004. Horizontal and vertical tree community structure in a lowland Atlantic rain forest, southeastern Brazil. Braz. J. Bot. 27 (4), 725–737.
Guisan, A., Zimmermann, N.E., 2000. Predictive habitat distribution models in ecology. Ecol. Model. 135 (2–3), 147–186.
Hall, F.G., Bergen, K., Blair, J.B., Dubayah, R., Houghton, R., Hurtt, G., Kellndorfer, J., Lefsky, M., Ranson, J., Saatchi, S., Shugart, H.H., Wickland, D., 2011. Characterizing 3D vegetation structure from space: mission requirements. Remote Sens. Environ. 115 (11), 2753–2775.
He, Q.S., Cao, C.X., Chen, E.X., Sun, G.Q., Ling, F.L., Pang, Y., Zhang, H., Ni, W.J., Xu, M., Li, Z.Y., Li, X.W., 2012. Forest stand biomass estimation using ALOS PALSAR data based on LiDAR-derived prior knowledge in the Qilian Mountain, western China. Int. J. Remote Sens. 33 (3), 710–729.
Helmer, E.H., Lefsky, M.A., Roberts, D.A., 2009. Biomass accumulation rates of Amazonian secondary forest and biomass of old-growth forests from Landsat time series and the Geoscience Laser Altimeter System. J. Appl. Remote Sens. 3 (1), 033505.
Hudak, A.T., Strand, E.K., Vierling, L.A., Byrne, J.C., Eitel, J.U.H., Martinuzzi, S., Falkowski, M.J., 2012. Quantifying aboveground forest carbon pools and fluxes from repeat LiDAR surveys. Remote Sens. Environ. 123 (1), 25–40.
Huete, A.R., Liu, H.Q., vanLeeuwen, W.J.D., 1997. The use of vegetation indices in forested regions: Issues of linearity and saturation. In: IGARSS '97 (Ed.) IEEE International Geoscience and Remote Sensing Symposium (IGARSS) Proceedings, vol. IV, Singapore, pp. 1966–1968.
IPCC, 2006. 2006 IPCC Guidelines for National Greenhouse Gas Inventories. In: Eggleston, H.S., Buendia, L., Miwa, K., Ngara, T., Tanabe, K. (Eds.), National Greenhouse Gas Inventories Programme. Institute for Global Environmental Strategies, Hayama Kanagawa (Japan).
IPCC, 2010. Expert Meeting on National Forest GHG Inventories. In: Eggleston, H.S., Srivastava, N., Tanabe, K., Baasansuren, J. (Eds.), National Forest GHG Inventories – a Stock Taking. Institute for Global Environmental Strategies, Hayama Kanagawa (Japan).
Kajisa, T., Murakami, T., Mizoue, N., Top, N., Yoshida, S., 2009. Object-based forest biomass estimation using Landsat ETM+ in Kampong Thom Province, Cambodia. J. For. Res. 14 (4), 203–211.
Kane, V., Gillespie, A., Mcgaughey, R., Lutz, J., Ceder, K., Franklin, J., 2008. Interpretation and topographic compensation of conifer canopy self-shadowing. Remote Sens. Environ. 112 (10), 3820–3832.
Li, H., Mausel, P., Brondizio, E., Deardorff, D., 2010. A framework for creating and validating a non-linear spectrum-biomass model to estimate the secondary succession biomass in moist tropical forests. ISPRS J. Photogramm. Remote Sens. 65 (2), 241–254.
Lira, P.K., Tambosi, L.R., Ewers, R.M., Metzger, J.P., 2012. Land-use and land-cover change in Atlantic Forest landscapes. For. Ecol. Manage. 278 (1), 80–89.
Liu, W., Song, C., Schroeder, T.A., Cohen, W.B., 2008. Predicting forest successional stages using multitemporal Landsat imagery with forest inventory and analysis data. Int. J. Remote Sens. 29 (13), 3855–3872.
Lu, D.S., 2006. The potential and challenge of remote sensing-based biomass estimation. Int. J. Remote Sens. 27 (7), 1297–1328.
Lu, D., Mausel, P., Brondizio, E., Moran, E., 2002. Assessment of atmospheric correction methods for Landsat TM data applicable to Amazon basin LBA research. Int. J. Remote Sens. 23 (13), 2651–2671.
Lu, D.S., Mausel, P., Brondizio, E., Moran, E., 2004. Relationships between forest stand parameters and Landsat TM spectral responses in the Brazilian Amazon Basin. For. Ecol. Manage. 198 (1–3), 149–167.
Main-Knorn, M., Moisen, G.G., Healey, S.P., Keeton, W.S., Freeman, E.A., Hostert, P., 2011. Evaluating the remote sensing and inventory-based estimation of biomass in the Western Carpathians. Remote Sens. 3 (7), 1427–1446.
Mantelli, L.R., Barbosa, J.M., Bitencourt, M.D., 2011. Assessing ecological risk through automated drainage extraction and watershed delineation. Ecol. Informatics 6 (5), 325–331.
Marques, M.C.M., Burslem, D.F.R.P., Britez, R.M., Silva, S.M., 2009. Dynamics and diversity of flooded and unflooded forests in a Brazilian Atlantic rain forest: a 16-year study. Plant Ecol. Divers. 2 (1), 57–64.
Martin, A.R., Thomas, S.C., 2011. A reassessment of carbon content in tropical trees. PLoS ONE 6 (8), e23533.
Mathys, L., Guisan, A., Kellenberger, T.W., Zimmermann, N.E., 2009. Evaluating effects of spectral training data distribution on continuous field mapping performance. ISPRS J. Photogramm. Remote Sens. 64 (6), 665–673.
McCullagh, P., Nelder, J.A., 1989. Generalized Linear Models, second ed. Chapman & Hall, London, UK.
Munroe, D.K., Nagendra, H., Southworth, J., 2007. Monitoring landscape fragmentation in an inaccessible mountain area: Celaque National Park, Western Honduras. Landscape Urban Plan. 83 (2–3), 154–167.
Myers, N., Mittermeier, R.A., Mittermeier, C.G., da Fonseca, G.A.B., Kent, J., 2000. Biodiversity hotspots for conservation priorities. Nature 403 (6772), 853–858.
Neeff, T., Lucas, R.M., Santos, J.R.d., Brondizio, E.S., Freitas, C.C., 2006. Area and age of secondary forests in Brazilian Amazonia 1978–2002: an empirical estimate. Ecosystems 9 (4), 609–623.
O'Brien, R.M., 2007. A caution regarding rules of thumb for variance inflation factors. Qual. Quant. 41 (5), 673–690.
Peroni, N., Hanazaki, N., 2002. Current and lost diversity of cultivated varieties, especially cassava, under swidden cultivation system in the Brazilian Atlantic Forest. Agric. Ecosyst. Environ. 92 (2–3), 171–183.
Pfaff, A., Walker, R., 2010. Regional interdependence and forest "transitions": substitute deforestation limits the relevance of local reversals. Land Use Policy 27 (2), 119–129.
Pontius, R.G., 2000. Quantification error versus location error in comparison of categorical maps. Photogramm. Eng. Remote Sens. 66 (8), 1011–1016.

Saatchi, S.S., Houghton, R.A., Dos Santos Alvalá, R.C., Soares, J.V., Yu, Y., 2007. Distribution of aboveground live biomass in the Amazon basin. Glob. Change Biol. 13 (4), 816–837.

Saatchi, S., Marlier, M., Chazdon, R.L., Clark, D.B., Russell, A.E., 2011. Impact of spatial variability of tropical forest structure on radar estimation of aboveground biomass. Remote Sens. Environ. 115 (11), 2836–2849.

Sarker, L.R., Nichol, J.E., 2011. Improved forest biomass estimates using ALOS AVNIR-2 texture indices. Remote Sens. Environ. 115 (4), 968–977.

Schwarz, M., Zimmermann, N.E., 2005. A new GLM-based method for mapping tree cover continuous fields using regional MODIS reflectance data. Remote Sens. Environ. 95 (4), 428–443.

Silva, W.G.d., Metzger, J.P., Bernacci, L.C., Catharino, E.L.M., Durigan, G., Simões, S., 2008. Relief influence on tree species richness in secondary forest fragments of Atlantic Forest, SE, Brazil. Acta Bot. Brasilica 22 (2), 589–598.

Sirén, A.H., Brondizio, E.S., 2009. Detecting subtle land use change in tropical forests. Appl. Geogr. 29 (2), 201–211.

Slater, P.N., 1980. Remote Sensing: Optics and Optical Systems. Addison-Wesley, Reading MA, USA.

Soenen, S.A., Peddle, D.R., Coburn, C.A., 2005. SCS+C: a modified sun-canopy-sensor topographic correction in forested terrain. IEEE Trans. Geosci. Remote Sens. 43 (9), 2148–2159.

Soenen, S.A., Peddle, D.R., Hall, R.J., Coburn, C.A., Hall, F.G., 2010. Estimating aboveground forest biomass from canopy reflectance model inversion in mountainous terrain. Remote Sens. Environ. 114 (7), 1325–1337.

SOS Mata Atlântica, 2012. Atlas dos remanescentes florestais da Mata Atlântica, período de 2010 a 2011. Instituto Nacional de Pesquisas Espaciais (INPE). <http://www.sosmatatlantica.org.br> (accessed 05.11.13).

Southworth, J., Tucker, C., 2001. The influence of accessibility, local institutions, and socioeconomic factors on forest cover change in the mountains of western Honduras. Mountain Res. Develop. 21 (3), 276–283.

Steininger, M.K., 2000. Satellite estimation of tropical secondary forest above-ground biomass: data from Brazil and Bolivia. Int. J. Remote Sens. 21 (6–7), 1139–1157.

Sun, G., Ranson, K.J., Kharuk, V.I., 2002. Radiometric slope correction for forest biomass estimation from SAR data in the Western Sayani Mountains, Siberia. Remote Sens. Environ. 79 (2–3), 279–287.

Tabarelli, M., Mantovani, W., 1999. A riqueza de espécies arbóreas na floresta atlântica de encosta no estado de São Paulo (Brasil). Rev. Brasileira Bot. 22 (2), 217–223.

Tangki, H., Chappell, N.A., 2008. Biomass variation across selectively logged forest within a 225-km^2 region of Borneo and its prediction by Landsat TM. For. Ecol. Manage. 256 (11), 1960–1970.

Teillet, P.M., Guindon, B., Goodenough, D.G., 1982. On the slope-aspect correction of multispectral scanner data. Can. J. Remote Sens. 8 (2), 84–106.

Teixeira, A.M.G., Soares, B.S., Freitas, S.R., Metzger, J.P., 2009. Modeling landscape dynamics in an Atlantic Rainforest region: implications for conservation. For. Ecol. Manage. 257 (4), 1219–1230.

Valeriano, M.d.M., 2008. TOPODATA: guia para utilização de dados geomorfológicos locais, INPE-15318-RPQ/818. Instituto Nacional de Pesquisas Espaciais (INPE), São José dos Campos SP, Brazil.

Valeriano, M.d.M., 2011. Cálculo do fator topográfico de iluminação solar para modelagem ecofisiológica a partir do processamento de Modelos Digitais de Elevação (MDE). In: INPE (Ed.), XV Simpósio Brasileiro de Sensoriamento Remoto, Instituto Nacional de Pesquisas Espaciais (INPE), Curitiba PR, Brazil, pp. 5933–5940.

Valeriano, M.d.M., Albuquerque, P.C.G.d., 2010. TOPODATA: processameto dos dados SRTM, INPE-16702-RPQ/854. Instituto Nacional de Pesquisas Espaciais (INPE), São José dos Campos SP, Brazil.

Valeriano, M.D., Rossetti, D.D., 2012. Topodata: Brazilian full coverage refinement of SRTM data. Appl. Geogr. 32 (2), 300–309.

Valeriano, M.M., Kuplich, T.M., Storino, M., Amaral, B.D., Mendes Jr, J.N., Lima, D.J., 2006. Modeling small watersheds in Brazilian Amazonia with shuttle radar topographic mission-90m data. Comput. Geosci. 32 (8), 1169–1181.

Vieira, I.C.G., de Almeida, A.S., Davidson, E.A., Stone, T.A., Reis de Carvalho, C.J., Guerrero, J.B., 2003. Classifying successional forests using Landsat spectral properties and ecological characteristics in eastern Amazônia. Remote Sens. Environ. 87 (4), 470–481.

Vieira, S.A., Alves, L.F., Aidar, M., Araújo, L.S., Baker, T., Batista, J.L.F., Campos, M.C., Camargo, P.B., Chave, J., Delitti, W.B.C., Higuchi, N., Honorio, E., Joly, C.A., Keller, M., Martinelli, L.A., De Mattos, E.A., Metzker, T., Phillips, O., Santos, F.A.M., Shimabukuro, M.T., Silveira, M., Trumbore, S.E., 2008. Estimation of biomass and carbon stocks: the case of the Atlantic Forest. Biota Neotropica 8 (2), 21–29.

Walker, R., 2012. The scale of forest transition: Amazonia and the Atlantic forests of Brazil. Appl. Geogr. 32 (1), 12–20.

Wang, C., Qi, J., 2008. Biophysical estimation in tropical forests using JERS-1 SAR and VNIR imagery. II. Aboveground woody biomass. Int. J. Remote Sens. 29 (23), 6827–6849.

Wijaya, A., Liesenberg, V., Gloaguen, R., 2010. Retrieval of forest attributes in complex successional forests of Central Indonesia: modeling and estimation of bitemporal data. For. Ecol. Manage. 259 (12), 2315–2326.

Wu, J., Bauer, M.E., Wang, D., Manson, S.M., 2008. A comparison of illumination geometry-based methods for topographic correction of QuickBird images of an undulant area. ISPRS J. Photogramm. Remote Sens. 63 (2), 223–236.

Zolkos, S.G., Goetz, S.J., Dubayah, R., 2013. A meta-analysis of terrestrial aboveground biomass estimation using lidar remote sensing. Remote Sens. Environ. 128 (1), 289–298.